Combined Measurements of Field Effect, Surface Photo-Voltage and Photoconductivity

By W. H. BRATTAIN and C. G. B. GARRETT

(Manuscript received May 10, 1956)

Combined measurements have been made of surface recombination velocity, surface photo-voltage, and the modulation of surface conductance and surface recombination velocity by an external field, on etched germanium surfaces. Two samples, cut from an n-type and a p-type crystal of known body properties, were used, the samples being exposed to the Brattain-Bardeen cycle of gaseous ambients. The results are interpreted in terms of the properties of the surface space-charge region and of the fast surface states. It is found that the surface barrier height, measured with respect to the Fermi level, varies from −0.13 to +0.13 volts, and that the surface recombination velocity varies over about a factor of ten in this range. From the measurements, values are found for the dependence of charge trapped in fast surface states on barrier height and on the steady-state carrier concentration within the semiconductor.

I. INTRODUCTION

This and the succeeding paper are concerned with studies of the properties of fast surface states on etched germanium surfaces. The experiments involve simultaneous measurement of a number of different physical surface properties. The theory, which will be presented in the second paper, interprets the results in terms of a distribution of fast surface states in the energy gap. The distribution function, and the cross-sections for transitions from the states into the conduction and valence bands, may then be deduced from the experimental results.

Early experiments[1] on contact potential of germanium, and on the change of contact potential with light, indicated that there are two kinds of surface charge associated with a germanium surface, over and above the holes and electrons that are distributed through the surface space-charge region. One kind of surface charge, usually called "charge

in fast traps" can follow a change in the space-charge region very fast in comparison with the light-chopping time used in that work ($\frac{1}{100}$ sec); the other kind, imagined to be more closely connected with adsorbed chemical material, can only change rather slowly. In a previous paper by the authors[2] it was pointed out that the Brattain-Bardeen experiments, taken by themselves, do not furnish unambiguous information concerning the distribution of these "fast" traps, but that such information might be obtained by performing, simultaneously, other measurements on the germanium surface. More recently Brown and Montgomery[3, 4] have provided a valuable tool in their studies of large-signal field effect; they point out that if, under given chemical conditions, it is possible to apply a field, normal to the surface, large enough to force the surface potential to the minimum in surface conductivity; then it becomes possible to determine the initial surface potential absolutely (provided certain considerations as to the mobility[5] of the carriers near the surface are valid).

This paper concerns studies of a number of physical properties that depend on the distribution and other characteristics of the surface traps or "fast" states. Measurements are reported of (i) the change of conductivity of a sample with field; (ii) the photoconductivity; (iii) the change of photoconductivity with field; (iv) the filament lifetime; and (v) the surface photo-voltage. Measurements were made in a series of gaseous ambients, first described by Brattain and Bardeen.[1] Evidence is presented to the effect that the variation in gas ambient changes only the "slow" states, leaving the distribution and other properties of the traps substantially unaffected. From measurements (i) to (iii) it is possible to construct the whole field-effect curve (conductance versus surface charge), even though the fields used were in general not large enough to reach the minimum in conductance.

Using the field effect data, values for the surface potential Y in units of kT/e could be obtained at each point, and also of the quantity $(\partial\Sigma_s/\partial Y)_{\delta=0}$, where Σ_s is the charge in surface traps, and the suffix $\delta = 0$ implies zero illumination. From measurements (ii) and (iv), the surface recombination velocity s could be deduced. (A more detailed study of photoconductivity in relation to surface recombination velocity will be reported at a later date.) Combined with the field effect data, this enables one to deduce the relation between s and Y.

Measurements of the surface photo-voltage may be presented in terms of the quantity $dY/d\delta$, where δ is equal to $\Delta p/n_i$, Δp being the density of added carrier-pairs in the body of the material, and n_i the intrinsic carrier density. The quantity $dY/d\delta$ is closely related to the ratio of the

change in surface potential produced by illumination of the surface to the change in the quasi-Fermi level for minority carriers. By measuring $dY/d\delta$ rather than dY/dL, discussed in Reference 2, the surface recombination velocity is eliminated from the surface photo-voltage data: the limiting values of $dY/d\delta$, after correction for the Dember effect, ought to be (p_0/n_i) and $-(n_i/p_0)$, no matter what the surface recombination velocity may be.

By combining this information with the field-effect data, one can deduce the quantity $(\partial\Sigma_s/\partial\delta)_Y$. This and the previous differential, deduced directly from the field-effect data, completely define the dependence of charge in surface traps on the two independent parameters Y and δ — that is, the dependence on chemical environment and on the bulk non-equilibrium carrier level.

The further interpretation of the quantities $(\partial\Sigma_s/\partial Y)_{\delta=0}$, $(\partial\Sigma_s/\partial\delta)_Y$ and s in terms of the distribution of surface traps is postponed to the succeeding paper. Here it is sufficient to say that the results are consistent with the assumption that the traps responsible for surface recombination are also those pertinent to the field effect and surface photovoltage experiments. Then the quantity $(\partial\Sigma_s/\partial Y)_{\delta=0}$ depends only on an integral over the distribution in energy of traps; $(\partial\Sigma_s/\partial\delta)_Y$ depends also on the ratios of cross-sections for transitions to the valence and conduction bands; and s depends in addition on the geometric mean cross-sections.

II. OUTLINE OF THE EXPERIMENT

The experiment is carried out with a slice of germanium, 0.025 cm thick, which is supported in such a way that there is a gap 0.025 cm wide between the slice and a metal plate. Substantially ohmic contacts are attached to the ends of the slice. Three kinds of experiment are now carried out:

(i) The conductance of the slice is modulated by illuminating it with a short flash of light; the subsequent decay of photoconductivity with time is studied, and the time-constant of the exponential tail measured.

(ii) A sinusoidally varying potential difference of about 500 volts peak-to-peak is applied between the metal plate and the germanium. Facilities are available for measuring the changes in conductance produced by the field. The sample is also illuminated with light chopped at a frequency different from that of the applied field. One measures: (a) the magnitude of the peak-to-peak conductance change in the dark; (b) the same in the presence of the light; and (c) the change in con-

conduction or the valence band. This in turn depends both on the surface potential and on the ratio of cross-sections for transitions to the two bands. For $Y \ll -1$, one expects $(\partial\Sigma_s/\partial\delta)_Y/(\partial\Sigma_s/\partial Y)_\delta$ to have the value $-\lambda^{-1}$; for $Y \gg +1$, the value $+\lambda$. These limiting values may be deduced by a somewhat general argument.[7]

At some intermediate value of surface potential, the above ratio must change sign. If the distribution of surface states in energy is known from the field effect measurements, then the value of Y at which the above ratio changes sign determines the ratio of cross-sections for those traps which are close to the Fermi level for that value of Y. By repeating the experiment for samples of differing bulk resistivity, it is then possible to determine whether the same ratio holds for the states at some different position in the energy gap.

III. EXPERIMENTAL DETAILS

Fig. 1 shows the experimental arrangements. The sample of germanium, of dimensions shown, was prepared by cutting, sandblasting, etching in CP4[1] and washing in distilled water. The exposed faces were approximately (100). The end contacts were made by sandblasting and soldering. The slots A, A' in the ceramic were incorporated in order to

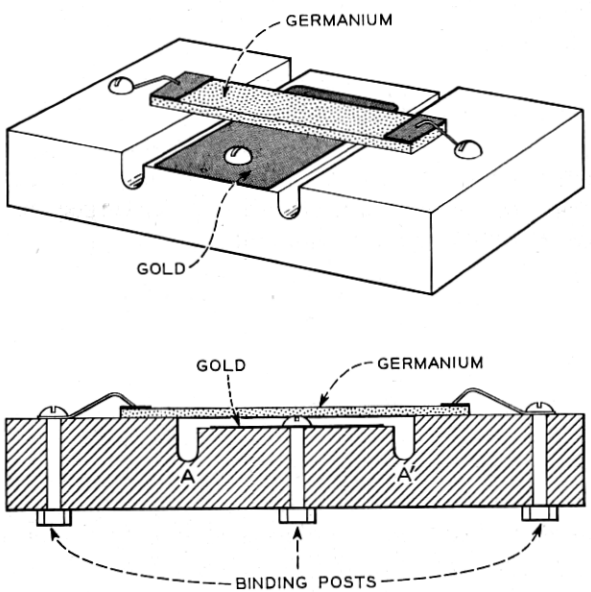

Fig. 1 — Experimental arrangement.

reduce the high field that would otherwise be present near the edges of the ceramic. The gold electrode was deposited by evaporation through a mask. Connections from the gold and from the ends of the sample were made to binding posts passing through the ceramic block.

The ceramic block was set into a metal box, divided into two compartments. In the upper compartment, which contained the sample, there were inlet and outlet tubes, to allow the gas to be changed. The lower compartment contained electrical components, which were thereby protected to a large extent from the changes in gas in the upper compartment. Facilities were available for the type of cycle of gas environment described by Brattain and Bardeen,[1] which cycle was found by them to produce reversible cyclic changes in surface potential. In the top of the box was a window, through which light could be shone onto the germanium either from a chopped or a flash source.

The electrical circuit is shown in Fig. 2. The condenser C_1 is that formed between the germanium and the gold, and has a capacity of about 2 $\mu\mu F$. Impedances Z_1 and Z_2 form a Wagner ground, which has to be balanced first. Then, by adjusting resistance R_1 and condenser C_2, one may obtain a balance in the case that there is no dc flowing through the sample. A current (determined by the battery B and the

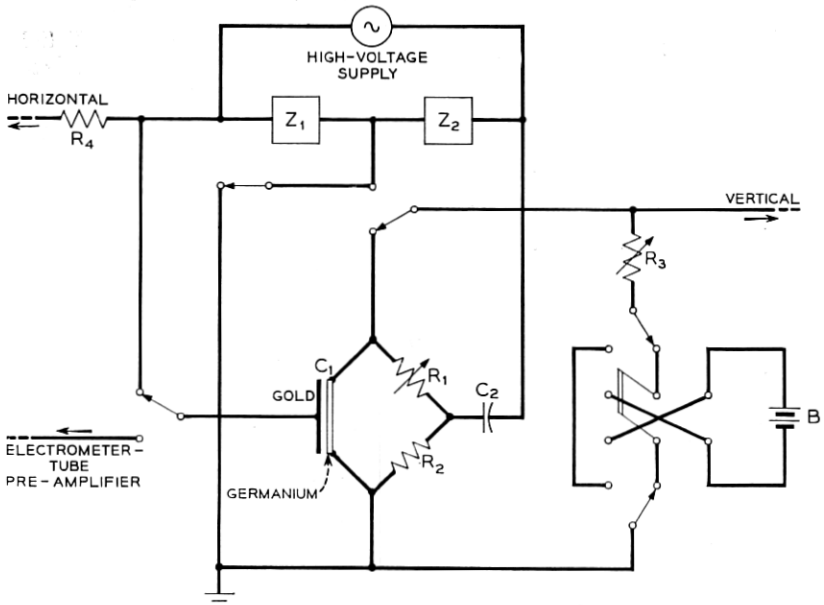

Fig. 2 — Electrical circuit.

resistance R_3) is now switched in, and the resulting off-balance (representing the field modulation of conductivity) presented on the vertical plates of an oscilloscope. The supply voltage is connected, via the high bleeder resistance R_4, to the horizontal plates. The frequency of the oscillator was chosen to be 25 cyc/sec, a value sufficiently low to obviate lifetime difficulties; the peak-to-peak swing was generally 500 volts.

During a field-effect measurement, the sample was also illuminated with light chopped at 90 cyc/sec. This had the result of causing to be presented on the oscilloscope screen a pattern such as that shown in Fig. 3. The lower tilted line represents the (dark) field effect curve; the vertical separation represents the photoconductivity, as modified by the applied field. Measurements were made of the mean vertical separation, and of the slopes of the upper and lower lines (by reading gain settings).

During a surface photo-voltage measurement, the gold electrode was disconnected from the high-voltage supply, and connected to a high-impedance detector, similar to that used in the work of Brattain and Bardeen.[1] A value for the chopped light intensity was chosen to give a contact potential change that was generally not more than 5 mV. A simultaneous measurement of the photoconductivity was also made.

The gas cycle was similar to that described by Brattain and Bardeen.[1] Some variations were made in it to try to spread out the rate of change with time so that the data could be obtained without large gaps. The cycle used was: (i) sparked oxygen 1 min, (ii) dry O_2, (iii) mixture of dry and wet O_2, (iv) wet O_2, (v) wet N_2, (vi) a mixture of dry and wet N_2, (vii) dry O_2, (viii) dry O_2, triple flow, and (ix) ozone normal flow. The normal rate of gas flow was about 2 liters per minute; the wet gas was obtained by bubbling through water (probably about 90 per

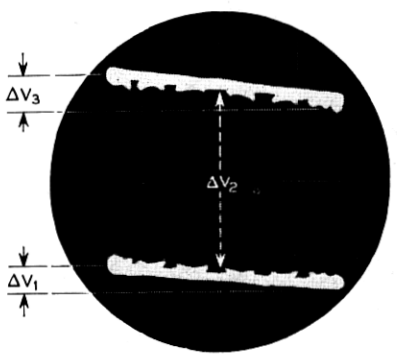

Fig. 3 — Picture of field effect-photoconductivity pattern, as observed on oscilloscope. Dark curve at the bottom.

cent r.h.) and the mixture of dry and wet was obtained by letting approximately one-half the gas flow bubble through H_2O. In carrying out the experiment, it was found convenient to carry out alternately a complete cycle of field effect and surface photo-voltage measurements. The values of the photoconductivity at equivalent points in successive cycles could be compared, in order to check that no systematic error was introduced by this procedure.

In addition to the foregoing, the following measurements were made:

1. All dimensions were determined.
2. The resistivity of the sample was found, and also the body lifetime, on another specimen cut from the same crystal.
3. The amplitude of the voltage swing was measured.
4. The amplifiers in the field effect circuit were calibrated.
5. The capacity of the germanium-gold condenser was determined (by a substitutional method). The value obtained was larger than that calculated from the parallel-plate formula, because of the edge effects.
6. A standard square-wave voltage was introduced into the surface photo-voltage circuit, in order to calibrate the high-impedance detector.
7. At several points in the cycle, the fundamental mode lifetime of the sample was determined by the photoconductivity decay method. This calibrated the 90 cyc/sec photoconductivity measurements, without the necessity for a knowledge of the light intensity.

IV. RESULTS

Measurements were made on two samples: one n-type, 22.6 ohm cm ($\lambda = 0.345$), the other p-type, 8.1 ohm cm ($\lambda = 17.7$). The body lifetime for both samples was greater than 10^{-3} sec, so that for slices of the thickness used (0.025 cm. or less), and for values of s in the range encountered, body recombination may be ignored.

Results of typical field-effect runs for the two samples are indicated in Tables I and II. The first column in each table gives the time in minutes from the beginning of the cycle at which the measurements were made. The second column shows the "effective mobility," $d\Delta G/d\Sigma$, obtained from the observed (dark) field effect signal voltage ΔV_1 (see Fig. 3) by use of the formula: $\mu_{\text{eff}} = w^2t^2\Delta V_1/I\rho_0{}^2CV_{\text{app}}$, where w is the width of the slice, t the thickness, I the dc flowing through it, ρ_0 the resistivity, C the capacity of the germanium-gold condenser, and V_{app} the voltage applied across it. The third column shows the mean value of $\delta(=\Delta p/n_i)$, obtained from the mean photoconductivity signal voltage

TABLE I — 22.6 OHM CM n-TYPE CYCLE 12.
RELATIVE LIGHT INTENSITY 0.082

Time min.	μ_{eff} $\frac{cm^2}{volt\ sec}$	δ	μ_{eff}^* $\frac{cm^2}{volt\ sec}$	s $\frac{cm}{sec}$
0	Sparked O_2			
1	Changed to dry O_2			
1.5	334	7.85×10^{-2}	520	90
2.5	344	6.9×10^{-2}	585	103
5.5	344	6.2×10^{-2}	595	114
6.5	344	6.07×10^{-2}	595	117
7.0	Changed to mixture of dry & wet O_2			
7.5	136	4.4×10^{-2}	520	161
8.5	84	4.02×10^{-2}	440	177
9.0	52	3.60×10^{-2}	270	196
10.0	Changed to full wet O_2			
11.0	−660	2.26×10^{-2}	−440	314
11.5	−890	1.74×10^{-2}	−780	408
12.0	−960	1.67×10^{-2}	−910	425
13.0	Changed to full wet N_2			
18.0	Changed to mixture of dry & wet N_2			
19.5	−1150	1.67×10^{-2}	−1060	425
20.5	−1050	1.74×10^{-2}	−960	408
22.5	−990	1.83×10^{-2}	−890	390
23.0	Changed to dry O_2			
23.5	−430	2.98×10^{-2}	−220	238
23.8	−290	3.2×10^{-2}	0	222
24.0	−84	3.81×10^{-2}	240	186
24.5	31	4.3×10^{-2}	310	165
26.5	146	4.7×10^{-2}	410	151
27.0	Tripled flow of dry O_2			
27.5	220	5.1×10^{-2}	450	139
29.5	260	5.7×10^{-2}	510	124
31.5	280	6.2×10^{-2}	510	114
35.0	Changed to ozone			
35.5	310	6.8×10^{-2}	510	104
37.5	320	8.2×10^{-2}	490	87

ΔV_2 by use of the formula: $\delta = wt\rho_i \Delta V_2 / I \ell_{ill} \rho_0^2$, where ρ_i is the intrinsic resistivity and ℓ_{ill} the length of the illuminated part of the slice. The fourth column shows the apparent effective mobility in the presence of light,* obtained from the field effect signal voltage ΔV_3 in the presence of light, using the same formula as that giving μ_{eff}. The last column shows the surface recombination velocity, which is proportional to δ^{-1} for fixed light intensity, the constant of proportionality being determined by comparison with measurements of the fundamental mode lifetime.

The results of typical surface photo-voltage runs are shown in Tables

* One must be careful to avoid thinking of μ_{eff}^* as a true field effect mobility, since it is really a sum of two quite different components: the true field effect mobility μ_{eff}, and a term, proportional to thickness of the slice, arising from the photoconductivity.

TABLE II — 8.1 OHM CM *p*-TYPE CYCLE 5.
RELATIVE LIGHT INTENSITY 0.25

Time min.	μ_{eff} $\frac{cm^2}{volt\ sec}$	δ	μ_{eff}^* $\frac{cm^2}{volt\ sec}$	s $\frac{cm}{sec}$
0	Started sparked O_2			
1.0	Changed to dry O_2			
1.5	307	4.1×10^{-2}	490	503
3.5	318	3.2×10^{-2}	490	660
6.0	Changed to mixture of wet & dry O_2			
7.5	273	1.4×10^{-2}	376	1480
9.5	239	1.3×10^{-2}	320	1580
11.0	Changed to wet O_2			
11.5	94	1.2×10^{-2}	−194	1690
12.5	−200	1.1×10^{-2}	−230	1820
15.5	−216	1.2×10^{-2}	−285	1690
17.0	Changed to wet N_2			
18.5	−352	1.6×10^{-2}	−570	1310
22.0	Changed to mixture of wet & dry O_2			
25.0	−80	1.1×10^{-2}	−137	1820
26.5	0	1.2×10^{-2}	31	1690
27.5	3.3	1.3×10^{-2}	58	1630
28.0	Changed to dry O_2			
29.0	193	1.9×10^{-2}	330	1070
29.5	239	2.2×10^{-2}	400	1000
30.5	250	2.4×10^{-2}	420	873
33.0	Tripled flow of dry O_2			
33.5	296	3.2×10^{-2}	500	645
34.5	296	3.7×10^{-2}	525	560
36.5	296	4.2×10^{-2}	570	490
37.5	296	4.6×10^{-2}	570	455
38.0	Changed to ozone			
42.5	330	6.4×10^{-2}	535	323

III and IV. Values of δ were obtained from the photoconductivity signal, as before, taking the actual illuminated length as the length of the sample. In making use of the standard square-wave calibration for the surface photo-voltage measurement (Section III), it is necessary to allow for the fact that the measured capacity involves the whole length of the sample, plus end and side fringing effects, whereas the surface photo-voltage measurements involves only the illuminated length, plus the fringe effect at the *sides*.

The penultimate column in Tables III and IV shows the ratio of the change in contact potential, measured in units of (kT/e), to the added-carrier parameter δ, which was deduced from the photoconductivity. This is not yet, however, the true surface photo-voltage function $(dY/d\delta)$, since the observed change in contact potential includes also the Dember potential ΔV_i[10] which occurs between the illuminated and non-illuminated parts of the *body* of the semiconductor. The last column in Tables III and IV shows the true values of $(dY/d\delta)$, obtained by sub-

TABLE III — 22.6 OHM CM n-TYPE CYCLE 7

Time mins.	Relative Light Intensity	δ	ΔCP volts	$\frac{\beta\Delta CP}{\delta}$	$\frac{dY}{d\delta}$
			Starting condition wet N_2		
6.5	2.25	0.36	6.5×10^{-3}	0.7	−0.10
11.5	2.25	0.34	1.0	0.115	−0.045
12.0	Changed to mixture wet and dry N_2				
12.5	2.25	0.32	2.2	0.27	0.10
13.0	2.25	0.34	3.5	0.40	0.23
13.5	2.25	0.35	4.6	0.51	0.34
14.5	2.25	0.38	6.8	0.70	0.53
15.5	0.56	0.10	3.1	1.2	1.03
17.5	0.56	0.11	3.7	1.33	1.16
18.0	Changed to dry O_2				
18.5	0.56	0.16	5.7	1.4	1.2
19.5	0.14	0.06	3.4	2.2	2.0
22.0	Changed to dry O_2 triple flow				
24.5	0.14	0.082	6.1	2.9	2.7

TABLE IV — 8.1 OHM CM p-TYPE CYCLE 8

Time mins.	Relative Light Intensity	δ	ΔCP volts	$\frac{\beta\Delta CP}{\delta}$	$\frac{dY}{d\delta}$
			Starting condition wet N_2		
0	Changed to mixture wet and dry N_2				
0.5	0.14	0.011	-3.5×10^{-3}	−12.5	−12.6
1.0	0.14	0.0088	−2.1	−9.6	−9.7
5.0	Changed to mixture wet and dry O_2				
5.5	0.56	0.0275	−1.8	−2.6	−2.7
6.0	0.56	0.03	−1.45	−1.9	−2.0
7.5	0.56	0.0325	−1.16	−1.4	−1.5
9.5	0.56	0.035	−1.08	−1.2	−1.3
10.0	Changed to dry O_2				
10.5	0.56	0.044	−0.71	−0.63	−0.69
11.5	0.56	0.055	−0.49	−0.35	−0.41
14.0	Changed to dry O_2 triple flow				
14.5	0.56	0.0625	−0.32	−0.20	−0.26
16.5	2.25	0.28	−0.72	−0.10	−0.16
20.5	2.25	0.33	−0.42	−0.05	−0.11
30.0	Changed to ozone				
31.5	2.25	0.47	+0.47	+0.039	−0.023
32.5	2.25	0.53	+1.4	+0.103	+0.041

tracting from ($\beta\Delta$ c.p./δ) a Dember potential correction, given by $(b - 1)/(\lambda + b\lambda^{-1})$. (The boundaries of the illuminated region were sufficiently distant from the contacts for this formula to apply.)

Tables III and IV include only data from the second half of the cycle (wet N_2 → ozone), since the rate of change of Δ c.p. during that part of the first half in which dry oxygen was replaced by wet oxygen was too fast to follow.

The reproducibility of all the data from cycle to cycle was good. One surprising result is that the surface recombination velocity assumed its maximum value close to the "wet nitrogen" extreme for both p-type and n-type. This behavior is quite different from that reported by Brattain and Bardeen,[1] who found s to be constant within 20 per cent throughout the range and Stephenson and Keyes,[8] who found a maximum value sometimes at one end, sometimes at the other, and sometimes in the middle. There is quite good agreement on the other hand, with the results of Many et al.[12], who report a maximum in s near the wet end of the cycle. The result of Brattain and Bardeen is not understood at the present time, and is probably wrong. The differences between the present work and that of Stephenson and Keyes may be associated with differences in surface preparation.

V. ANALYSIS OF THE RESULTS

From now onwards we shall express all experimental and calculated quantities in terms of the following dimensionless ratios:

$$\bar{\Gamma}_p = \Gamma_p/n_i\mathfrak{L} \qquad \bar{\Gamma}_n = \Gamma_n/n_i\mathfrak{L}$$
$$\bar{\Sigma}_s = \Sigma_s/en_i\mathfrak{L} \qquad \bar{\Sigma} = \bar{\Sigma}_s + \bar{\Gamma}_p - \bar{\Gamma}_n \tag{2}$$
$$\overline{\Delta G} = \Delta G/en_i\mu_p\mathfrak{L}, \qquad \bar{\mu}_{\text{eff}} = \mu_{\text{eff}}/\mu_p\,, \qquad \bar{\mu}_{\text{eff}}{}^* = \mu_{\text{eff}}{}^*/\mu_p$$

where ΔG is the surface conductance, $\mathfrak{L}$ the Debye length for intrinsic germanium (1.4×10^{-4} cm), and μ_p is the mobility for holes (1800 cm^2v^{-1} sec^{-1}). Tables V and VI show values of the quantities we shall need, as functions of the surface potential Y, calculated from the theoretical considerations of Garrett and Brattain.[2] The surface conductance, and the differentials in the fifth and sixth columns, are evaluated for $\delta = 0$.

TABLE V — 22.6 OHM CM n-TYPE

Y	$Y - \ln\lambda$	$\bar{\Gamma}_p - \bar{\Gamma}_n$	$\Delta\bar{G}$	$\left(\frac{\partial(\bar{\Gamma}_p - \bar{\Gamma}_n)}{\partial Y}\right)_\delta$	$\left(\frac{\partial(\bar{\Gamma}_p - \bar{\Gamma}_n)}{\partial\delta}\right)_Y$
3	4.1	−10.3	17.5	−4.1	−1.3
2	3.1	−7.0	10.6	−2.6	−0.8
1	2.1	−4.9	6.2	−1.8	−0.4
0	1.1	−3.4	3.3	−1.3	0.0
−1	0.1	−2.3	1.45	−1.1	0.5
−2	−0.9	−1.2	0.36	−1.1	1.3
−3	−1.9	0.0	0.0	−1.4	2.7
−4	−2.9	1.7	0.65	−2.1	5.2
−5	−3.9	4.4	2.65	−3.5	9.4
−6	−4.9	8.9	6.8	−5.8	16.3
−7	−5.9	16.4	14.4	−9.5	27.7

TABLE VI — 8.1 OHM CM p-TYPE

Y	$Y - \ln\lambda$	$\bar{\Gamma}_p - \bar{\Gamma}_n$	$\Delta\bar{G}$	$\left(\frac{\partial(\bar{\Gamma}_p - \bar{\Gamma}_n)}{\delta Y}\right)_\delta$	$\left(\frac{\partial(\bar{\Gamma}_p - \bar{\Gamma}_n)}{\partial\delta}\right)_Y$
8	5.1	−8	9.8	−5.5	−87
7	4.1	−4	3.4	−3.1	−42
6	3.1	−2	0.8	−1.9	−19
5	2.1	0	0.0	−1.45	−8.2
4	1.1	1	0.25	−1.3	−3.4
3	0.1	2	1.3	−1.45	−1.5
2	−0.9	4	2.8	−1.75	−0.62
1	−1.9	6	4.8	−2.4	−0.21
0	−2.9	9	7.4	−3.4	0.0
−1	−3.9	12	10.9	−4.3	0.15
−2	−4.9	18	16.4	−6.4	0.31
−3	−5.9	26	25.0	−10.0	0.53

The first problem is the constructing, from the experimental results, of the curve relating $\overline{\Delta G}$ and $\bar{\Sigma}$. The experiments provide a series of pic tures like Fig. 3, each one corresponding to a different chemical environment, and so to a different Y. At each of two succeeding pictures of this sort one knows (i) the vertical displacement (photoconductivity) between the dark and light field effect curves; and (ii) the mean difference in the dark and light slopes, and hence the rate of change of photoconductivity with applied field, and therefore with $\bar{\Sigma}$. The problem is to deduce the horizontal displacement (in $\bar{\Sigma}$) between the two pictures.

A corrrection must first be made for the fact that the ambient changes $\bar{\Sigma}$ uniformly on both surfaces, whereas the applied field induces charge only on the lower surface, plus fringing effects.* The correction is applied by taking the difference in slopes ($\mu_{\text{eff}}{}^* - \mu_{\text{eff}}$), and multiplying this by (2/1.27), where the number 1.27 is deduced for the given geometry from the standard edge-effect formula.[9] This having been done, it is now possible to take the revised pictures and piece them together to form two smooth curves (Fig. 4). The process of assembling such a diagram determines the horizontal and vertical distances, and therefore the change of $\bar{\Sigma}$ and $\overline{\Delta G}$, between successive experiments.

This argument may be given analytically as follows. First notice that the photoconductivity voltage in the absence of field (ΔV_2 in Fig. 3) is proportional to $(1/s)$. The application of a voltage between the gold and the germanium induces some charge density Σ at each point on the germanium surface, Σ being (due to fringing effects) a complicated function of position. At each point $(1/s)$ is changed by an amount $\Sigma[d(1/s)/d\Sigma]$. This causes the photoconductivity in the presence of field

* We are indebted to W. L. Brown for bringing this to our attention.

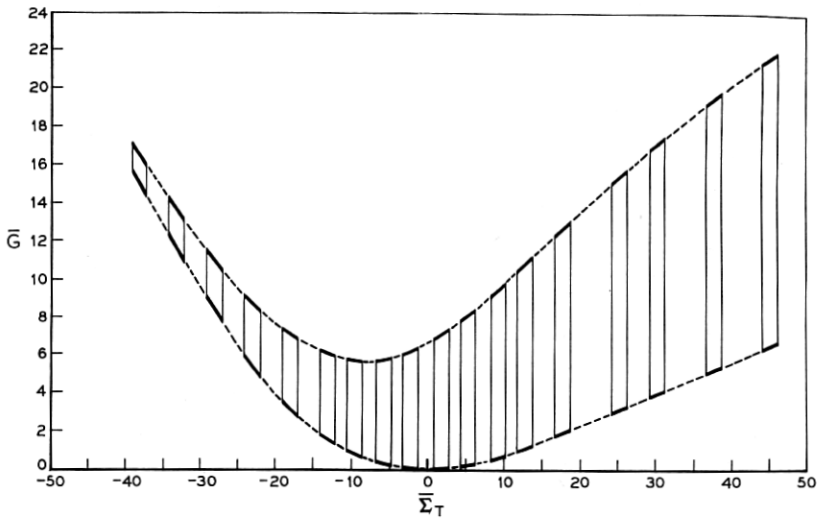

Fig. 4 — Construction of the curve relating $\Delta\overline{G}$ (surface conductivity, in units of $e\mu_p n_i \mathfrak{L}$) and $\overline{\Sigma}$ (surface charge, in units of $en_i\mathfrak{L}$).

to differ from that in zero field, and gives rise to the voltage difference $(\Delta V_3 - \Delta V_1)$ shown in Fig. 3. Expressing this difference in terms of the difference $(\mu_{\text{eff}}{}^* - \mu_{\text{eff}})$ between the apparent and true effective mobilities in the presence of light (see Section IV), one finds:

$$(\mu_{\text{eff}}{}^* - \mu_{\text{eff}}) = \left(\frac{w^2t^2}{I\rho_0{}^2C}\right) K \frac{d(1/s)}{d\Sigma} \left(\frac{C_{\text{unit}}}{2w}\right) \tag{3}$$

where K is the constant of proportionality between $(1/s)$ and the photoconductivity signal ΔV_2, and C_{unit} is the capacity per unit of the germanium-gold condenser in the illuminated region, which is 1.27 times the parallel-plate formula. From a series of measurements of $(\mu_{\text{eff}}{}^* - \mu_{\text{eff}})$ and ΔV_2 it is now possible to obtain $\overline{\Sigma}$ by graphical integration:

$$\Sigma = \left(\frac{1}{en_i\mathfrak{L}}\right)\left(\frac{w^2t^2}{I\rho_0{}^2C}\right)\left(\frac{C_{\text{unit}}}{2w}\right) \int \frac{d\Delta V_2}{\mu_{\text{eff}}{}^* - \mu_{\text{eff}}} \tag{4}$$

This and the graphical method are of course equivalent. It is worthwhile emphasizing again that either technique depends for its validity on the fact that the distribution of fast states is unaffected by the gas changes in the Brattain-Bardeen cycle, as shown in the experiments of Brown and Montgomery.[4] If, however, the assumption were too far from the truth, the fitting of *both* slopes in Fig. 4 would be impossible. The only

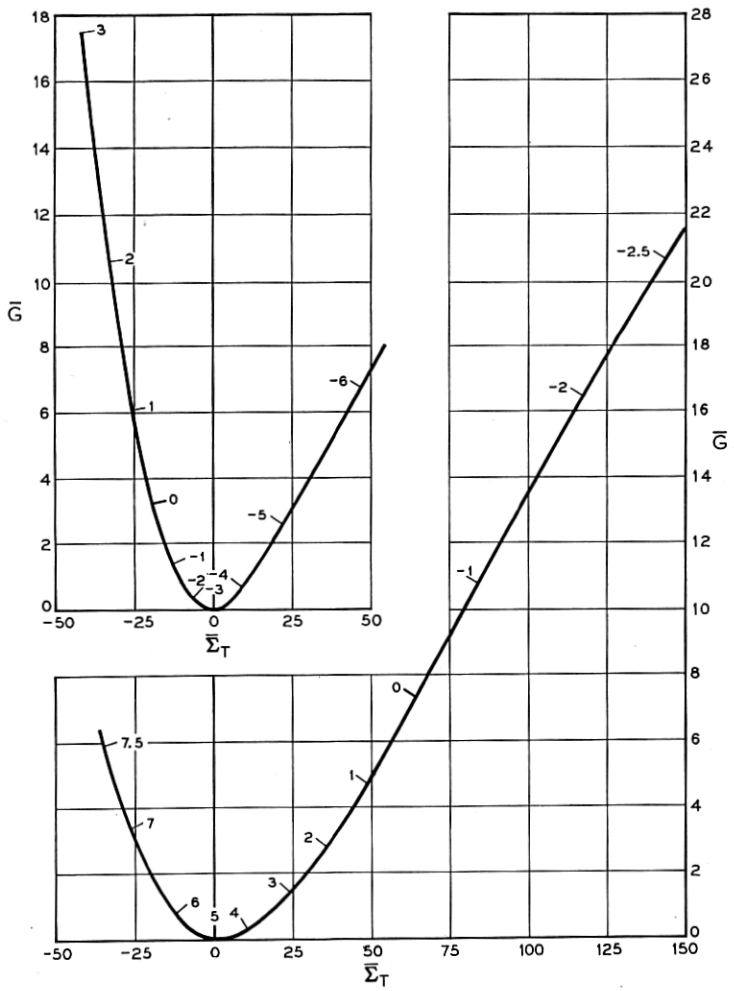

Fig. 5 — Curves showing $\Delta\overline{G}$ (surface conductivity, in units of $e\mu_p n_i \mathfrak{L}$) and $\overline{\Sigma}$ surface charge, in units of $en_i\mathfrak{L}$) for the 22.6 ohm-cm sample (upper curve) and for the 8.1 ohm-cm sample (lower curve). Values of Y, deduced from the surface conductivity, are indicated on the curves.

place at which fitting was at all difficult was at the extreme wet end. For most of the range, therefore, the method is at least internally consistent.

Fig. 5 shows the result of carrying out this procedure for the n and p-type samples. The data were averaged over a number of runs. The numbers appearing on the curves represent values of Y, obtained by reference to Tables V and VI.

From Fig. 5 one may now calculate[4] the changes occurring in $\bar{\Sigma}_s$, the (reduced) charge in fast states, since $\bar{\Gamma}_p - \bar{\Gamma}_n$ may be read from Tables V and VI, and $\bar{\Sigma}_s = \bar{\Sigma} - (\bar{\Gamma}_p - \bar{\Gamma}_n)$. Fig. 6 shows $(\partial\bar{\Sigma}_s/\partial Y)_\delta$ as a function of $Y - \ln\lambda$, calculated from the experimental results in this way. [The reason for plotting against $Y - \ln\lambda$ instead of Y is that this quantity represents the difference, in units of (kT/e), between the electrostatic potential at the surface and the Fermi level. In this way the effects of difference from sample to sample in the position of the Fermi level in the interior are eliminated.] Notice that the measurements of $(\partial\bar{\Sigma}_s/\partial Y)_\delta$ for the two samples have the same general shape, and that the turning points of the two curves occur at about the same value of

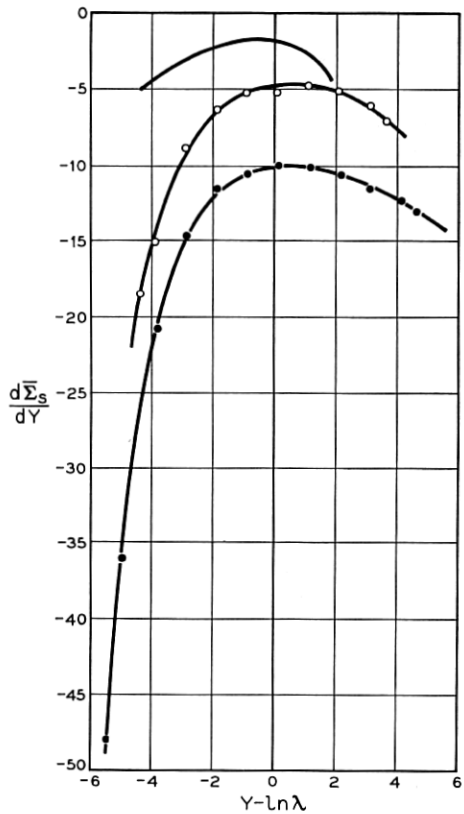

Fig. 6 — Differential charge in fast states versus surface potential. The graphs show $(\partial\bar{\Sigma}_s/\partial Y)$ plotted against $Y - \ln\lambda$. Dots: p-type; circles: n-type. A typical result of Brown and Montgomery, using 28 ohm-cm p-type germanium, is also shown.

$(Y - \ln \lambda)$. Fig. 7 shows the variation of surface recombination velocity with $Y - \ln \lambda$, using the experimental photoconductivity data and values of Y read from Fig. 5. The values of s have been divided by $(\lambda + \lambda^{-1})$, as indicated, since $s/(\lambda + \lambda^{-1})$ is expected to be the same, at a given value of $(Y - \ln \lambda)$, for all samples, so long as the distribution of fast states is the same. The agreement shown in Fig. 7 is probably closer than would be expected in the light of the experimental accuracy.

Fig. 8 shows the observed dependence of $dY/d\delta$ on $(Y - \ln \lambda)$ for both samples, using the data of Tables III and IV, and using the photoconductivity to determine, from Fig. 7, the value of Y at each point. On the figure the expected limiting values ($-\lambda$ and λ^{-1}) are shown for both samples. Of the four asymptotes, the higher limit of $(dY/d\delta)$ for the n-type sample is satisfactorily reached for large negative values of Y; the experimental values for the p-type sample appear to be approaching the expected limit for large positive values of Y, while the information regarding the approach to the two lower limits is too fragmentary to do more than show that the order of magnitude is as expected. Now taking the data shown in Fig. 8, making use of (1) and the calculations given in Tables III and IV, one calculates $(\partial \bar{\Sigma}_s/\partial \delta)_Y/(\partial \bar{\Sigma}_s/\partial Y)_\delta$. The values so found are plotted against Y in Fig. 9. Fig. 6, 7 and 9, showing the observed variation of $(\partial \bar{\Sigma}_s/\partial Y)_\delta$, s and $(\partial \bar{\Sigma}_s/\partial \delta)_Y/(\partial \bar{\Sigma}_s/\partial Y)_\delta$ with Y, furnish a complete description of the properties of the fast states at the

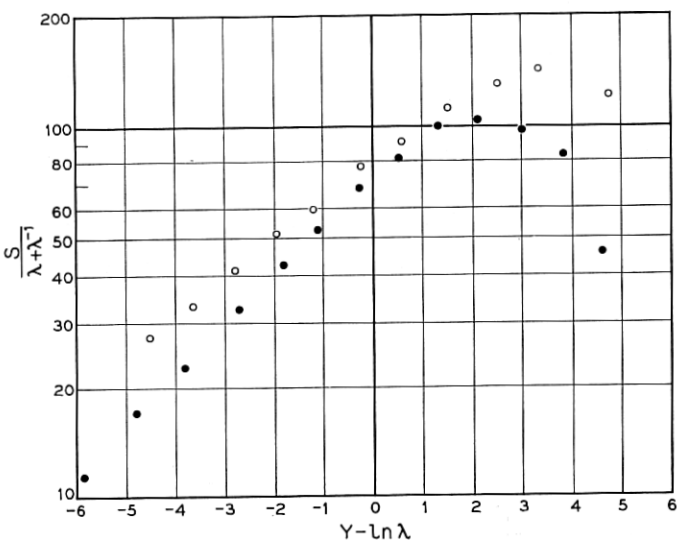

Fig. 7 — Surface recombination velocity versus surface potential. The curves show $s/(\lambda + \lambda^{-1})$ plotted against $Y - \ln \lambda$. Dots: p-type; circles: n-type.

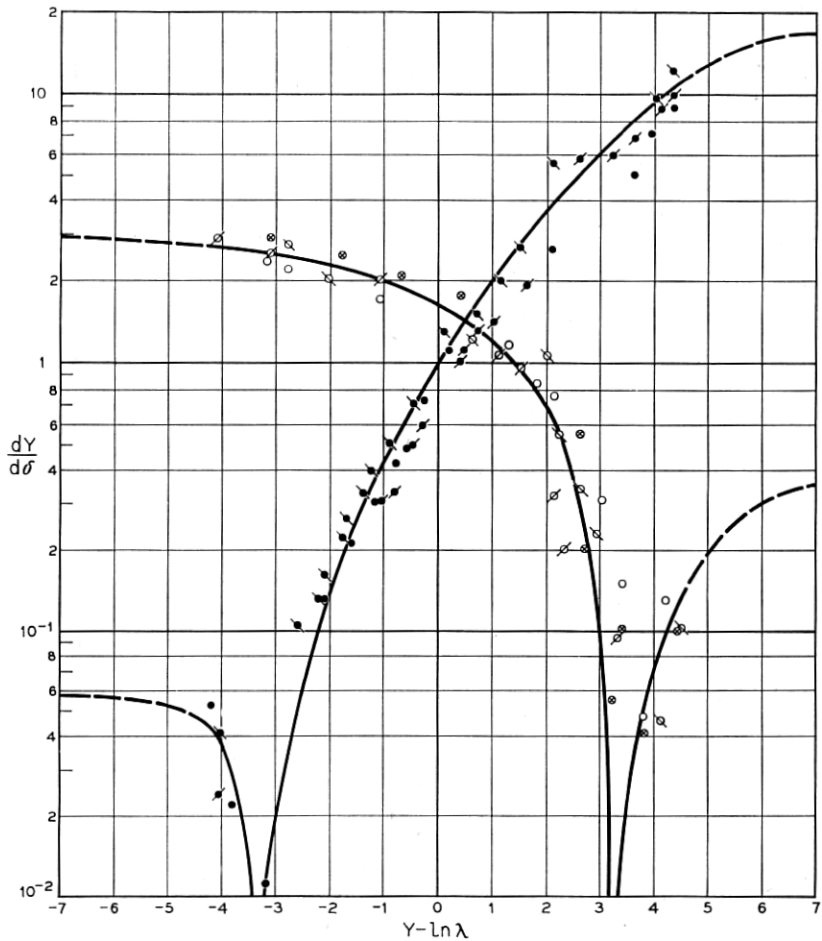

Fig. 8 — Surface photo-voltage (change in contact potential in relation to added carrier concentration). $dY/d\delta$ is shown plotted against $Y - \ln \lambda$. Dots: p-type; circles: n-type. Data from different runs are distinguished by modifications to these symbols. The left-hand branches denote absolute magnitudes, since the ratio is negative there. At the extreme left hand of the diagram, the fast states near to the Fermi level are in good contact with the valence band: at the extreme right hand, to the conduction band. The theoretical asymptotes (λ^{-1} to the left and λ to the right) are also indicated.

temperature studied. This is the basic information which any theoretical treatment must explain. In the succeeding paper this matter is discussed from the point of view of the statistics of a distribution of fast states, and information on the cross sections, as well as on the distribution itself, is derived from the data just presented.

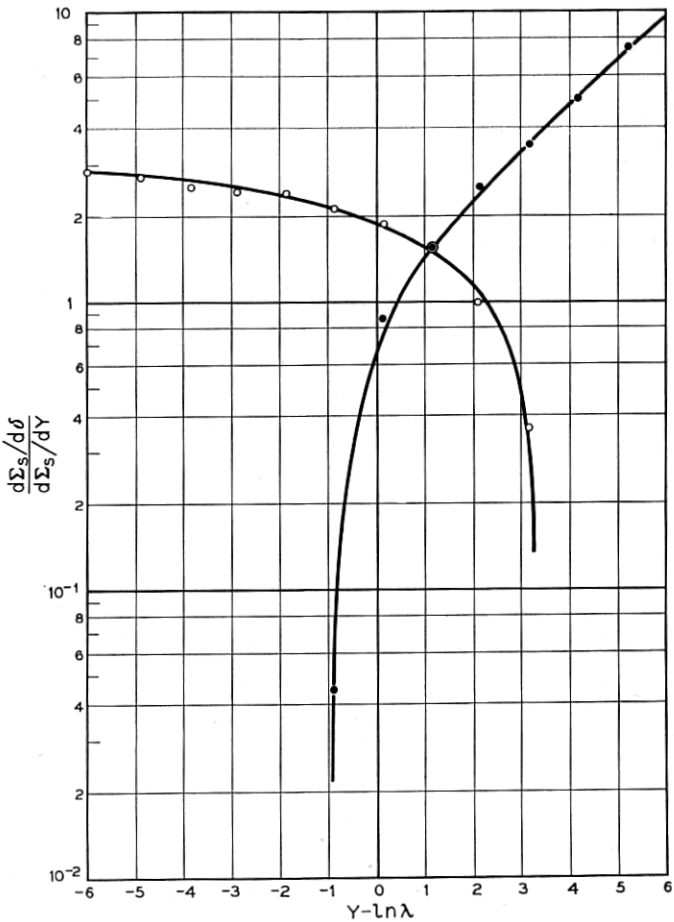

FIG. 9 — The function $(\partial\bar{\Sigma}_s/\partial\delta)Y/(\partial\bar{\Sigma}_s/\partial Y)_\delta$ plotted against $Y - \ln\lambda$. Dots: p-type; circles: n-type.

VI. FURTHER COMMENTS

The development given in the previous section has concerned particularly the properties of the fast states. As to the slow states, the experiments are much less informative. The variations of Y with gas are generally consistent with the variations of contact potential previously reported,[1] although the total range in Y (± 0.13 volt) is smaller by about a factor of 2 than that in contact potential found in the previous work. One must say that roughly half the change of contact potential is in V_B, (i.e., βY) and half in V_D, the potential drop across the ion layer.

It may be seen from the figures that it is the quantity $(Y - \ln \lambda)$, rather than Y, which appears to be characteristic of the point in the cycle reached. This property of a semiconductor surface, and possible reasons therefore, have often been discussed in the literature.[11] The total range of surface potential is illustrated in Fig. 10, which is drawn to scale, and also shows sundry other points of interest found in the present research. The potential diagrams for n-type and p-type are drawn with the Fermi levels aligned, to show the relation between the property $(Y - \ln \lambda) =$ const. and the frequently observed smallness of the contact potential difference between n and p-type germanium.

As to the reproducibility and accuracy of the work presented here, the following points may be of interest: (i) The measurements were repeated on another n-type sample of nearly the same resistivity as the one reported here, but cut from a different crystal. The results on this sample were indistinguishable, within the experimental error, from those found on the first n-type sample. (ii) If the sample was re-etched in precisely the same way as before, and the experiments repeated, the results were in good agreement with those obtained before. However, variations in the etching procedure sometimes gave quite different re-

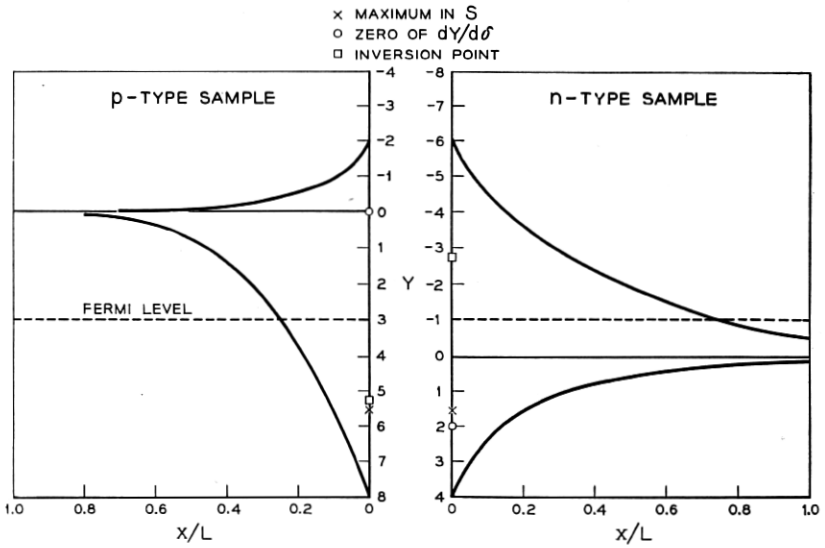

Fig. 10 — The shapes of the surface space-charge regions for the p-type and n-type samples in the extremes of gaseous environment. The two surfaces are to the center of the figure. The solid curves show the center of the gap (intrinsic Fermi level) plotted against distance, in units of an intrinsic Debye length. Also shown are the positions of the zeros of $(dY/d\delta)$, the maxima of s, and the minima of surface conductivity.

sults. We hope to discuss this at a future date. (iii) The accuracy of the measurements is not high. Some of the more directly-derivable quantities, such as s, should be known to 5 per cent, but a quantity like $(\partial\overline{\Sigma}_s/\partial\delta)/(\partial\overline{\Sigma}_s/\partial Y)$, which is only obtained after a long and elaborate calculation involving a number of corrections, is perhaps uncertain to 30 per cent.

VII. CONCLUSIONS

This paper has presented results of combined measurements of field effect, photoconductivity, change of photoconductivity with field, filament lifetime and surface photo-voltage, on slices of germanium. From the measurements, the surface potential Y has been found at each point, and the variations of the quantities $(\partial\overline{\Sigma}_s/\partial Y)$, s and $(\partial\overline{\Sigma}_s/\partial\delta)/(\partial\overline{\Sigma}_s/\partial Y)$ with Y determined.

It is a pleasure to record our thanks to W. L. Brown, for comments on field effect techniques and many stimulating discussions, to H. R. Moore, who constructed the high-voltage power supply, and to A. A. Studna, who assisted in the experiments. We are also grateful to C. Herring for comments on the text.

BIBLIOGRAPHY

1. W. H. Brattain and J. Bardeen, Surface Properties of Germanium, B.S.T.J., **32,** pp. 1–41, Jan. 1953.
2. C. G. B. Garrett and W. H. Brattain, Physical Theory of Semiconductor Surfaces, Phys. Rev., **99,** pp. 376–387, July 15, 1955.
3. W. L. Brown, Surface Potential and Surface Charge Distribution from Semiconductor Field Effect Measurements, Phys. Rev., **98,** p. 1565, June 1, 1955.
4. H. C. Montgomery and W. L. Brown, Field-Induced Conductivity Changes in Germanium, Phys. Rev., **103,** Aug. 15, 1956.
5. J. R. Schrieffer, Effective Carrier Mobility in Surface Charge Layers, Phys. Rev., **97,** pp. 641–646, Feb. 1, 1955.
6. C. G. B. Garrett and W. H. Brattain, Interfacial Photo-Effects in Germanium at Room Temperature, Proc. of the Conference on Photo Conductivity, Nov., 1954, Wiley, in press.
7. W. H. Brattain and C. G. B. Garrett, Surface Properties of Germanium and Silicon, Ann. N. Y. Acad. of Science, **58,** pp. 951–958, Sept., 1954.
8. D. T. Stevenson and R. J. Keyes, Measurements of Surface Recombination Velocity at Germanium Surfaces, Physica, **20,** pp. 1041–1046, Nov., 1954.
9. J. Clerk Maxwell, Electricity and Magnetism, 3rd Edition, **1,** p. 310, Clarendon Press, 1904.
10. W. van Roosbroeck, Theory of Photomagnetoelectric Effect in Semiconductors, Phys. Rev., **101,** pp. 1713–1725, March 15, 1956.
11. J. Bardeen and S. R. Morrison, Surface Barriers and Surface Conduction, Physica, **20,** p. 873, 1954.
12. E. Harnik, A. Many, Y. Margoninski and E. Alexander, Correlation Between Surface Recombination Velocity and Surface Conductivity in Germanium, Phys. Rev., **101,** pp. 1434–1435, Feb. 15, 1956.